

1 **OPTIMAL NEURAL NETWORK APPROXIMATION OF**
2 **WASSERSTEIN GRADIENT DIRECTION OF KL DIVERGENCE VIA**
3 **CONVEX OPTIMIZATION***

4 YIFEI WANG[†], PENG CHEN[‡], MERT PILANCI[†], AND WUCHEN LI[§]

5 **Abstract.** The calculation of the direction of the Wasserstein gradient is vital for addressing
6 problems related to posterior sampling and scientific computing. To approximate the Wasserstein
7 gradient using finite samples, it is necessary to solve a variation problem. Our study focuses on
8 the variation problem within the framework of two-layer networks with squared-ReLU activations.
9 We present a semi-definite programming (SDP) relaxation as a solution, which can be viewed as
10 an approximation of the Wasserstein gradient for a broader range of functions, including two-layer
11 networks. By solving the convex SDP, we achieve the best approximation of the Wasserstein gra-
12 dient direction in this function class. We also provide conditions to ensure the relaxation is tight.
13 Additionally, we propose methods for practical implementation, such as subsampling and dimension
14 reduction. The effectiveness and efficiency of our proposed method are demonstrated through nu-
15 merical experiments, including Bayesian inference with PDE constraints and parameter estimation
16 in COVID-19 modeling.

17 **Key words.** Bayesian inference, Convex Optimization, Neural Network, Semi-positive Definite
18 Program.

19 **MSC codes.** 62F15, 41A30, 65K10

20 **1. Introduction.** Bayesian inference is a crucial method for determining model
21 parameters based on observational data. It is widely used in fields such as inverse
22 problems, scientific computing, information science, and machine learning [46]. The
23 core issue in Bayesian inference is obtaining samples from a posterior distribution,
24 which describes the distribution of parameters based on both data and prior informa-
25 tion.

26 The Wasserstein gradient flow, as first introduced in references such as [41, 2, 28],
27 has been proven to be an efficient method for obtaining samples from a posterior
28 distribution. This has led to growing interest in recent years. For example, the
29 Wasserstein gradient flow of the Kullback-Leibler (KL) divergence is related to over-
30 damped Langevin dynamics. Discretizing the overdamped Langevin dynamics results
31 in the classical Langevin Monte Carlo Markov Chain (MCMC) algorithm. Therefore,
32 the computation of the Wasserstein gradient flow offers a unique perspective on sam-
33 pling algorithms. Additionally, the direction of the Wasserstein gradient also offers
34 a deterministic method for updating a particle system as demonstrated in [10]. A
35 number of efficient sampling algorithms have been developed by utilizing approxima-

*Submitted to the editors DATE.

Funding: W. Li is supported in part by AFOSR MURI FP 9550-18-1-502; in part by AFOSR YIP award No. FA9550-23-1-0087; and in part by the National Science Foundation (NSF) RTG: 2038080. P. Chen is partially supported by NSF DMS 2245674. Yifei Wang and Mert Pilanci was supported in part by the National Science Foundation (NSF) under Grant DMS-2134248; in part by the NSF CAREER Award under Grant CCF-2236829; in part by the U.S. Army Research Office Early Career Award under Grant W911NF-21-1-0242; and in part by the Office of Naval Research under Grant N00014-24-1-2164.

[†]Department of Electrical Engineering, Stanford University, Stanford, CA (wangyf18@stanford.edu, pilanci@stanford.edu).

[‡]School of Computational Science and Engineering, College of Computing, Georgia Institute of Technology, Atlanta, GA (pchen402@gatech.edu).

[§]Department of Mathematics, University of South Carolina, Columbia, SC (wuchen@mailbox.sc.edu).

tion or generalization of the Wasserstein gradient direction. Such examples include the Wasserstein gradient descent (WGD) with kernel density estimation (KDE) [35], Stein variational gradient descent (SVGD) [36], and neural variational gradient descent [15].

Neural networks have demonstrated impressive abilities in learning complex functions from data, as well as in Bayesian inverse problems [44, 40, 30, 32]. According to the universal approximation theorem of neural networks [23, 38], any complex function can be learned by a two-layer neural network with non-linear activations and a sufficient number of neurons. Furthermore, functions represented by neural networks provide a natural approximation to the Wasserstein gradient direction.

However, due to the nonlinear and nonconvex nature of neural networks, optimization algorithms such as stochastic gradient descent may not always find the global optimal solutions for the training problem. Recently, based on a line of research [42, 45, 4], the regularized training problem of two-layer neural networks with ReLU/polynomial activation and a convex loss function can be formulated as a convex program. By solving this convex program, it is possible to construct the entire set of global optima for the nonconvex training problem [52]. Theoretical analysis [51] has also shown that global optima of the training problem correspond to simpler models with better generalization properties. Numerical experiments have also shown that neural networks found by solving the convex program can achieve higher train accuracy and test accuracy compared to neural networks trained by SGD with the same number of parameters.

In this paper, we investigate a variational problem whose optimal solution corresponds to the Wasserstein gradient direction. Our focus is on the family of two-layer neural networks with squared ReLU activation. We formulate the regularized variational problem in terms of samples, and instead of directly training the neural network to minimize the loss, we analyze the convex dual problem of the training problem and study its semi-definite program (SDP) relaxation by analyzing the geometry of dual constraints. The resulting SDP can be efficiently solved by convex optimization solvers such as CVXPY [16]. We also analyze the choice of the regularization parameter and present a practical implementation using subsampling and dimension reduction to improve computational efficiency. Numerical experiments for PDE-constrained inference problems and Covid-19 parameter estimation problems demonstrate the effectiveness and efficiency of our method.

1.1. Related works. The time and spatial discretizations of Wasserstein gradient flows are extensively studied in literature [27, 28, 9, 10, 6, 37, 22]. Recently, neural networks have been applied in solving or approximating Wasserstein gradient flows [39, 34, 33, 1, 8, 24, 20]. For sampling algorithms, [15] learns the transportation function by solving an unregularized variational problem in the family of vector-output deep neural networks. Compared to these studies, we focus on a convex SDP relaxation of the variational problem induced by the Wasserstein gradient direction. Meanwhile, [21] form the Wasserstein gradient direction as the minimizer of the Bregman score and they apply deep neural networks to solve the induced variational problem. In short, we study the same variational problem but we focus on the two-layer neural networks, provide convex SDP relaxations and give sufficient conditions when the relaxation is exact.

In comparison to previous works on the convex optimization formulations of neural networks using SDP [4, 5], they focus on the polynomial activation and give the exact convex optimization formulation (instead of convex relaxation). In comparison, we

85 focus on the neural networks with the squared ReLU activation, which has not been
 86 considered before. Our method can also apply to the analysis of supervised learning
 87 problems using neural networks with squared ReLU activation. Moreover, previous
 88 works on the convex optimization formulation of neural networks mainly focus on the
 89 supervised learning problem of two-layer neural networks using convex loss functions
 90 (e.g., squared loss, logistic loss). Our work utilizes a similar convex analytic framework
 91 to solve the variational problem of approximating the Wasserstein gradient direction,
 92 which is different from supervised learning. The convex optimization approach is
 93 based on the idea of infinite-width neural networks modeled as probability measures.
 94 The dual problem itself is equivalent to the convex dual problem when the neural
 95 network in the primal problem has infinitely many neurons. However, the convex
 96 optimization approach tackles networks of arbitrary width that are able to learn useful
 97 representations, while the infinite width is often limited to kernel methods.

98 **2. Background.** In this section, we briefly review the Wasserstein gradient de-
 99 scent and present its variational formulation. In particular, we focus on the Wasser-
 100 stein gradient descent direction of KL divergence functional. Later on, we design a
 101 neural network convex optimization problem to approximate the Wasserstein gradient
 102 in samples.

103 **2.1. Wasserstein gradient descent.** Consider an optimization problem in the
 104 probability space:

$$105 \quad (2.1) \quad \inf_{\rho \in \mathcal{P}} D_{\text{KL}}(\rho \parallel \pi) = \int \rho(x)(\log \rho(x) - \log \pi(x))dx,$$

106 Here the integral is taken over \mathbb{R}^d and the objective functional $D_{\text{KL}}(\rho \parallel \pi)$ is the KL
 107 divergence from ρ to π . The variable is the density function ρ in the space $\mathcal{P} = \{\rho \in$
 108 $C^\infty(\mathbb{R}^d) \mid \int \rho dx = 1, \rho > 0\}$. The function $\pi \in C^\infty(\mathbb{R}^d)$ is a known probability density
 109 function of the posterior distribution. By solving the optimization problem (2.1), we
 110 can generate samples from the posterior distribution.

111 A known fact [47, Chapter 8.3.1] is that the Wasserstein gradient descent flow for
 112 the optimization problem (2.1) satisfies

$$113 \quad \begin{aligned} \partial_t \rho_t &= \nabla \cdot \left(\rho_t \nabla \frac{\delta}{\delta \rho_t} D_{\text{KL}}(\rho_t \parallel \pi) \right) \\ &= \nabla \cdot (\rho_t (\nabla \log \rho_t - \nabla \log \pi)) \\ &\stackrel{(a)}{=} \Delta \rho_t - \nabla \cdot (\rho_t \nabla \log \pi), \end{aligned}$$

114 where $\rho_t(x) = \rho(x, t)$, $\frac{\delta}{\delta \rho_t}$ is the L^2 first variation operator w.r.t. ρ_t , $\nabla \cdot F$ denotes the
 115 divergence of a vector valued function $F : \mathbb{R}^d \rightarrow \mathbb{R}^d$ and Δ is the Laplace operator.
 116 In step (a) we use the fact that $\rho_t \nabla \log \rho_t = \nabla \rho_t$. This equation is also known as
 117 the gradient drift Fokker-Planck equation. It corresponds to the following updates in
 118 terms of samples :

$$119 \quad (2.2) \quad dx_t = -(\nabla \log \rho_t(x_t) - \nabla \log \pi(x_t))dt.$$

120 Clearly, when $\rho_t = \pi$, the above dynamics reaches the equilibrium, which implies that
 121 the samples x_t are generated by the posterior distribution.

122 To solve the Wasserstein gradient flow (2.2), we consider a forward Eulerian dis-
 123 cretization in time. In the l -th iteration, suppose that $\{x_l^n\}$ are samples drawn from

124 ρ_l . The update rule of Wasserstein gradient descent (WGD) on the particle system
 125 $\{x_l^n\}$ follows

$$126 \quad (2.3) \quad x_{l+1}^n = x_l^n - \alpha_l \nabla \Phi_l(x_l^n),$$

127 where $\Phi_l : \mathbb{R}^d \rightarrow \mathbb{R}$ is a function which approximates $\log \rho_l - \log \pi$ and $\alpha_l > 0$ is the
 128 step size.

129 **2.2. Variational formulation of WGD.** Given the particles $\{x_n\}_{n=1}^N$, we de-
 130 sign the following variational problem to choose a suitable function Φ approximating
 131 the function $\log \rho - \log \pi$. Consider

$$132 \quad (2.4) \quad \inf_{\Phi \in C^1(\mathbb{R}^d)} \frac{1}{2} \int \|\nabla \Phi(x) - (\nabla \log \rho(x) - \nabla \log \pi(x))\|_2^2 \rho(x) dx.$$

133 The objective function evaluates the least-square discrepancy between $\nabla \log \rho - \nabla \log \pi$
 134 and $\nabla \Phi$ weighted by the density ρ . The optimal solution follows $\Phi = \log \rho - \log \pi$,
 135 up to a constant shift. Let $\mathcal{H} \subseteq C^1(\mathbb{R}^d)$ be a finite-dimensional function space. The
 136 following proposition gives a formulation of (2.4) in \mathcal{H} .

137 **PROPOSITION 2.1.** *Let $\mathcal{H} \subseteq C^1(\mathbb{R}^d)$ be a function space. The variational problem*
 138 *(2.4) in the domain \mathcal{H} can be reformulated to*

$$139 \quad (2.5) \quad \inf_{\Phi \in \mathcal{H}} \frac{1}{2} \int \|\nabla \Phi(x)\|_2^2 \rho dx + \int \Delta \Phi(x) \rho(x) dx \\ + \int \langle \nabla \log \pi(x), \nabla \Phi(x) \rangle \rho(x) dx.$$

140 *Proof.* We first note that

$$141 \quad (2.6) \quad \frac{1}{2} \int \|\nabla \Phi - \nabla \log \rho + \nabla \log \pi\|_2^2 \rho dx \\ = \frac{1}{2} \int \|\nabla \Phi\|_2^2 \rho dx + \int \langle \nabla \log \pi - \nabla \log \rho, \nabla \Phi \rangle \rho dx \\ + \frac{1}{2} \int \|\nabla \log \rho - \nabla \log \pi\|_2^2 \rho dx.$$

142 We notice that the term $\frac{1}{2} \int \|\nabla \log \rho - \nabla \log \pi\|_2^2 \rho dx$ does not depend on Φ . Utilizing
 143 the integration by parts, we can compute that

$$144 \quad (2.7) \quad \int \langle \nabla \log \rho, \nabla \Phi \rangle \rho dx = \int \left\langle \frac{\nabla \rho}{\rho}, \nabla \Phi \right\rangle \rho dx \\ = \int \langle \nabla \rho, \nabla \Phi \rangle dx \\ = - \int \Delta \Phi \rho dx.$$

145 Therefore, the variational problem (2.4) is equivalent to

$$146 \quad (2.8) \quad \inf_{\Phi \in C^1(\mathbb{R}^d)} \frac{1}{2} \int \|\nabla \Phi\|_2^2 \rho dx + \int \langle \nabla \log \pi, \nabla \Phi \rangle \rho dx + \int \Delta \Phi \rho dx.$$

147 By restricting the domain to \mathcal{H} , we complete the proof. \square

148 *Remark 2.2.* A similar variational problem has been studied in [15]. If we replace
 149 $\nabla\Phi$ for $\Phi \in \mathcal{H}$ by a vector field Ψ in a certain function family, then, the quantity
 150 in (2.5) is the negative regularized Stein discrepancy defined in [15] between ρ and
 151 π based on Ψ . This problem is also similar to the variational problem for the score
 152 matching estimator in [25] by parameterizing Φ in a given probabilistic model. In
 153 comparison, our method can be viewed as a special case of score matching by using a
 154 two-layer neural network.

155 Therefore, by replacing the density ρ by finite samples $\{x_n\}_{n=1}^N \sim \rho$, the problem
 156 (2.5) in terms of finite samples forms

$$157 \quad (2.9) \quad \inf_{\Phi \in \mathcal{H}} \frac{1}{N} \sum_{n=1}^N \left(\frac{1}{2} \|\nabla\Phi(x_n)\|_2^2 + \Delta\Phi(x_n) \right) \\ + \frac{1}{N} \sum_{n=1}^N \langle \nabla \log \pi(x_n), \nabla\Phi(x_n) \rangle.$$

158 **3. Optimal neural network approximation of Wasserstein gradient.** In
 159 this section, we focus on functional space \mathcal{H} of functions represented by two-layer neu-
 160 ral networks. We derive the primal and dual problems of the regularized Wasserstein
 161 variational problems. By analyzing the dual constraints, a convex SDP relaxation of
 162 the dual problem is obtained. We also present a practical implementation estimation
 163 of $\nabla \log \rho - \nabla \log \pi$ and discuss the choice of the regularization parameter.

164 Let ψ be an activation function. Consider the case where \mathcal{H} is a class of two-layer
 165 neural network with the activation function $\psi(x)$:

$$166 \quad (3.1) \quad \mathcal{H} = \{ \Phi_{\theta} \in C^1(\mathbb{R}^d) \mid \Phi_{\theta}(x) = \alpha^T \psi(W^T x) \},$$

167 where $\theta = (W, \alpha)$ is the parameter in the neural network with $W \in \mathbb{R}^{d \times m}$ and $\alpha \in \mathbb{R}^m$.

168 *Remark 3.1.* We can extend this model to handle by adding an entry of 1 in
 169 x_1, \dots, x_n .

170 For two-layer neural networks, we can compute the gradient and Laplacian of $\Phi \in \mathcal{H}$
 171 as follows:

$$172 \quad (3.2) \quad \nabla\Phi_{\theta}(x) = \sum_{i=1}^m \alpha_i w_i \psi'(w_i^T x) = W(\psi'(W^T x) \circ \alpha),$$

173

$$174 \quad (3.3) \quad \Delta\Phi_{\theta}(x) = \sum_{i=1}^m \alpha_i \|w_i\|_2^2 \psi''(w_i^T x).$$

175 Here \circ represents the element-wise multiplication. By adding a regularization term
 176 to the variational problem (2.9), we obtain

$$177 \quad (3.4) \quad \min_{\theta} \frac{1}{2N} \sum_{n=1}^N \left\| \sum_{i=1}^m \alpha_i w_i \psi'(w_i^T x_n) \right\|_2^2 \\ + \frac{1}{N} \sum_{n=1}^N \left\langle \sum_{i=1}^m \alpha_i w_i \psi'(w_i^T x_n), \nabla \log \pi(x_n) \right\rangle \\ + \frac{1}{N} \sum_{n=1}^N \sum_{i=1}^m \alpha_i \|w_i\|_2^2 \psi''(w_i^T x_n) + \frac{\beta}{2} R(\theta),$$

178 where $\beta > 0$ is the regularization parameter. We focus on the squared ReLU activation
 179 $\psi(z) = (z)_+^2 = (\max\{z, 0\})^2$. Note that a non-vanishing second derivative is required
 180 for the Laplacian term in (3.3), which makes the ReLU activation inadequate. For
 181 this activation function, we consider the regularization function $R(\boldsymbol{\theta}) = \sum_{i=1}^m (\|w_i\|_2^3 +$
 182 $|\alpha_i|^3)$.

183 *Remark 3.2.* We note that $\nabla\Phi_{\boldsymbol{\theta}}(x)$ and $\Delta\Phi_{\boldsymbol{\theta}}(x)$ are all piece-wise degree-3 poly-
 184 nomials of the parameters $\boldsymbol{\theta}$. Hence, we consider a specific cubic regularization term
 185 above, analogous to [4]. By choosing this regularization term, we can derive a simpli-
 186 fied dual problem.

187 By utilizing the arithmetic and geometric mean (AM-GM) inequality, we can
 188 rescale the first and second-layer parameters and formulate the regularized variational
 189 problem (3.4) as follows.

190 **PROPOSITION 3.3** (Primal problem). *The regularized variational problem (3.4)*
 191 *can be reformulated to*

$$\begin{aligned}
 & \min_{W, \alpha} \frac{1}{2} \sum_{n=1}^N \left\| \sum_{i=1}^m \alpha_i w_i \psi'(w_i^T x_n) \right\|^2 \\
 & + \sum_{n=1}^N \sum_{i=1}^m \alpha_i \|w_i\|_2^2 \psi''(w_i^T x_n) \\
 & + \sum_{n=1}^N \left\langle \sum_{i=1}^m \alpha_i w_i \psi'(w_i^T x_n), \nabla \log \pi(x_n) \right\rangle + \tilde{\beta} \|\alpha\|_1, \\
 & \text{s.t. } \|w_i\|_2 \leq 1, i \in [m],
 \end{aligned}
 \tag{3.5}$$

193 where $\tilde{\beta} = 3 \cdot 2^{-5/3} N \beta$ and we denote $[m] = \{1, \dots, m\}$.

194 *Proof.* Suppose that $\hat{w}_i = \beta_i^{-1} w_i$ and $\hat{\alpha}_i = \beta_i^2 \alpha_i$, where $\beta_i > 0$ is a scale parameter
 195 for $i \in [m]$. Let $\boldsymbol{\theta}' = \{(\hat{w}_i, \hat{\alpha}_i)\}_{i=1}^m$. We note that

$$\hat{\alpha}_i \hat{w}_i \psi'(\hat{w}_i^T x_n) = \beta_i \alpha_i w_i \psi'(\beta_i^{-1} w_i^T x_n) = \alpha_i w_i \psi'(w_i^T x_n),
 \tag{3.6}$$

197 and

$$\hat{\alpha}_i \|\hat{w}_i\|_2^2 \psi''(\hat{w}_i^T x_n) = \alpha_i \|w_i\|_2^2 \psi''(w_i^T x_n) = \alpha_i \|w_i\|_2^2 \psi''(w_i^T x_n).
 \tag{3.7}$$

199 This implies that $\Phi_{\boldsymbol{\theta}}(x) = \Phi_{\boldsymbol{\theta}'}(x)$ and $\nabla \cdot \Phi_{\boldsymbol{\theta}}(x) = \nabla \cdot \Phi_{\boldsymbol{\theta}'}(x)$. For the regularization
 200 term $R(\boldsymbol{\theta})$, we note that

$$\begin{aligned}
 & \|\hat{w}_i\|_2^3 + \|\hat{\alpha}_i\|_2^3 = \beta_i^6 |\alpha_i|^3 + \beta_i^{-3} \|w_i\|_2^3 \\
 & = \beta_i^6 |\alpha_i|^3 + \frac{1}{2} \beta_i^{-3} \|w_i\|_2^3 + \frac{1}{2} \beta_i^{-3} \|w_i\|_2^3 \\
 & = 3 \cdot 2^{-2/3} \|w_i\|_2^2 |\alpha_i|.
 \end{aligned}
 \tag{3.8}$$

202 The optimal scaling parameter is given by $\alpha_i = 2^{-1/9} \frac{\|w_i\|_2^{1/3}}{|\alpha_i|^{1/3}}$. As the scaling operation
 203 does not change $\|w_i\|_2^2 |\alpha_i|$, we can simply let $\|w_i\|_2 = 1$. Thus, the regularization term
 204 $\frac{\tilde{\beta}}{2} R(\boldsymbol{\theta})$ becomes $\frac{\tilde{\beta}}{N} \sum_{i=1}^m \|w_i\|_1$. This completes the proof. \square

205 In short, the optimal value of (3.4) and (3.5) are the same. We can obtain the
 206 optimal solution of (3.5) by rescaling the optimal solution of (3.4) and vice versa.

207 For simplicity, we write $Y \in \mathbb{R}^{N \times d}$ whose n -row is $\nabla \log \pi(x_n)$ for $n \in [N]$. We
 208 introduce the slack variable $z_n = \sum_{i=1}^m \alpha_i w_i \psi'(x_n^T w_i)$ for $n \in [N]$ and denote $Z =$
 209 $[z_1 \ \dots \ z_N]^T \in \mathbb{R}^{N \times d}$. Then, we can simplify the problem (3.5) to

$$\begin{aligned}
 & \min_{W, \alpha, Z} \frac{1}{2} \|Z\|_F^2 + \sum_{n=1}^N \sum_{i=1}^m \alpha_i \|w_i\|_2^2 \psi''(w_i^T x_n) \\
 & \quad + \text{tr}(Y^T Z) + \tilde{\beta} \|\alpha\|_1, \\
 & \text{s.t. } z_n = \sum_{i=1}^m \alpha_i w_i \psi'(x_n^T w_i), n \in [N], \\
 & \quad \|w_i\|_2 \leq 1, i \in [m].
 \end{aligned}
 \tag{3.9}$$

211 To derive the convex relaxation of the neural network training problem, the dual
 212 problem plays an important role. By applying the Lagrangian duality, we can derive
 213 the dual problem of (3.9) as follows.

214 **PROPOSITION 3.4** (Dual problem). *The dual problem of the regularized varia-*
 215 *tional problem (3.9) is*

$$\begin{aligned}
 & -\frac{1}{2} \|\Lambda + Y\|_F^2, \\
 & \text{s.t. } \max_{w: \|w\|_2 \leq 1} \left| \sum_{n=1}^N \|w\|_2^2 \psi''(x_n^T w) - \lambda_n^T w \psi'(x_n^T w) \right| \leq \tilde{\beta},
 \end{aligned}
 \tag{3.10}$$

217 which provides a lower-bound on (3.9). .

218 *Proof.* Consider the Lagrangian function

$$\begin{aligned}
 L(Z, W, \alpha, \Lambda) &= \frac{1}{2} \|Z\|_F^2 + \sum_{n=1}^N \sum_{i=1}^m \alpha_i \|w_i\|_2^2 \psi''(w_i^T x_n) + \text{tr}(Y^T Z) + \tilde{\beta} \|\alpha\|_1 \\
 & \quad + \sum_{n=1}^N \lambda_n^T \left(z_n - \sum_{i=1}^m \alpha_i w_i \psi'(x_n^T w_i) \right) \\
 &= \tilde{\beta} \|\alpha\|_1 + \sum_{i=1}^m \alpha_i \sum_{n=1}^N (\|w_i\|_2^2 \psi''(w_i^T x_n) - \lambda_n^T w_i \psi'(x_n^T w_i)) \\
 & \quad + \frac{1}{2} \|Z\|_F^2 + \text{tr}((Y + \Lambda)^T Z).
 \end{aligned}
 \tag{3.11}$$

220 For fixed W , the constraints on Z and α are linear and the strong duality holds. Thus,
 221 we can exchange the order of $\min_{Z, \alpha}$ and \max_{Λ} . Thus, we can compute that
 (3.12)

$$\begin{aligned}
 & \min_{W \in \mathcal{W}, Z, \alpha} \max_{\Lambda} L(Z, W, \alpha, \Lambda) \\
 &= \min_{W \in \mathcal{W}} \max_{\Lambda} \min_{\alpha, Z} L(Z, W, \alpha, \Lambda) \\
 &= \min_{W \in \mathcal{W}} \max_{\Lambda} \min_{\alpha, Z} \tilde{\beta} \|\alpha\|_1 + \sum_{i=1}^m \alpha_i \sum_{n=1}^N (\|w_i\|_2^2 \psi''(w_i^T x_n) - \lambda_n^T w_i \psi'(x_n^T w_i)) + \frac{1}{2} \|Z\|_F^2 + \text{tr}((Y + \Lambda)^T Z) \\
 &= \min_{W \in \mathcal{W}} \max_{\Lambda} -\frac{1}{2} \|\Lambda + Y\|_F^2 + \sum_{i=1}^m \mathbb{I} \left(\max_{w_i: \|w_i\|_2 \leq 1} \left| \sum_{n=1}^N \|w_i\|_2^2 \psi''(w_i^T x_n) - \lambda_n^T w_i \psi'(x_n^T w_i) \right| \leq \tilde{\beta} \right).
 \end{aligned}
 \tag{3.12}$$

223 By exchanging the order of min and max, we can derive the dual problem:
 (3.13)

$$\begin{aligned}
 & \max_{\Lambda} \min_{W \in \mathcal{W}} -\frac{1}{2} \|\Lambda + Y\|_F^2 + \sum_{i=1}^m \mathbb{I} \left(\max_{w_i: \|w_i\|_2 \leq 1} \left| \sum_{n=1}^N \|w_i\|_2^2 \psi''(w_i^T x_n) - \lambda_n^T w_i \psi'(x_n^T w_i) \right| \leq \tilde{\beta} \right) \\
 224 & = \max_{\Lambda} -\frac{1}{2} \|\Lambda + Y\|_F^2 \text{ s.t. } \max_{w_i: \|w_i\|_2 \leq 1} \left| \sum_{n=1}^N \|w_i\|_2^2 \psi''(w_i^T x_n) - \lambda_n^T w_i \psi'(x_n^T w_i) \right| \leq \tilde{\beta}, i \in [m] \\
 & = \max_{\Lambda} -\frac{1}{2} \|\Lambda + Y\|_F^2 \text{ s.t. } \max_{w: \|w\|_2 \leq 1} \left| \sum_{n=1}^N \|w\|_2^2 \psi''(w^T x_n) - \lambda_n^T w \psi'(x_n^T w) \right| \leq \tilde{\beta}, i \in [m]
 \end{aligned}$$

225 This completes the proof. \square

226 We note that the dual problem can be infeasible if the regularization parameter
 227 $\tilde{\beta}$ is below a certain threshold. In other words, if the regularization term is missing
 228 or the regularization parameter is not large enough, the optimal value of the dual
 229 problem is $-\infty$ and the primal problem is not lower bounded.

230 **3.1. Analysis of dual constraints and the relaxed dual problem.** Now,
 231 we analyze the constraint in the dual problem. We note that it is closely related
 232 to the regularization parameter, which we will discuss later. For simplicity, we take
 233 $\psi''(0) = 0$ as the subgradient of $\psi'(z)$ at $z = 0$, i.e., taking the left derivative of $\psi'(z)$
 234 at $z = 0$. Let $X = [x_1, \dots, x_N]^T \in \mathbb{R}^{N \times d}$. Denote the set of all possible hyper-plane
 235 arrangements corresponding to the rows of X as

$$236 \quad (3.14) \quad \mathcal{S} = \{\text{diag}(\mathbb{I}(Xw \geq 0)) \mid w \in \mathbb{R}^d, w \neq 0\}.$$

237 Here $\mathbb{I}(s) = 1$ if the statement s is correct and $\mathbb{I}(s) = 0$ otherwise. Let $p = |\mathcal{S}|$ be
 238 the cardinality of \mathcal{S} , and write $\mathcal{S} = \{D_1, \dots, D_p\}$. According to [12], we have the
 239 upper bound $p \leq 2r \binom{e(N-1)}{r}$, where $r = \text{rank}(X)$. Based on the analysis of the
 240 dual constraints, we can derive a convex SDP as a relaxed dual problem.

241 **PROPOSITION 3.5** (Relaxed dual problem). *The relaxed dual problem is the fol-*
 242 *lowing SDP:*

$$\begin{aligned}
 & \max_{\Lambda, \{r^{(j,-)}, r^{(j,+)}\}_{j=1}^p} -\frac{1}{2} \|\Lambda + Y\|_F^2, \\
 243 \quad (3.15) \quad & \text{s.t. } \tilde{A}_j(\Lambda) + \tilde{B}_j + \sum_{n=0}^N r_n^{(j,-)} H_n^{(j)} + \tilde{\beta} e_{d+1} e_{d+1}^T \succeq 0 \\
 & -\tilde{A}_j(\Lambda) - \tilde{B}_j + \sum_{n=0}^N r_n^{(j,+)} H_n^{(j)} + \tilde{\beta} e_{d+1} e_{d+1}^T \succeq 0 \\
 & r^{(j,+)} \geq 0, r^{(j,-)} \geq 0, j \in [p],
 \end{aligned}$$

244 where we denote $[p] = \{1, \dots, p\}$. For $j \in [p]$, we denote $A_j(\Lambda) = -\Lambda^T D_j X - X^T D_j \Lambda$,
 245 $B_j = 2 \text{tr}(D_j) I_d$, $\tilde{A}_j(\Lambda) = \begin{bmatrix} A_j(\Lambda) & 0 \\ 0 & 0 \end{bmatrix}$, $\tilde{B}_j = \begin{bmatrix} B_j & 0 \\ 0 & 0 \end{bmatrix}$, $H_0^{(j)} = \begin{bmatrix} I_d & 0 \\ 0 & -1 \end{bmatrix}$ and $H_n^{(j)} =$
 246 $\begin{bmatrix} 0 & (1 - 2(D_j)_{nn})x_n \\ (1 - 2(D_j)_{nn})x_n^T & 0 \end{bmatrix}$, $n \in [N]$ The vector $e_{d+1} \in \mathbb{R}^{d+1}$ satisfies that
 247 $(e_{d+1})_i = 0$ for $i \in [d]$ and $(e_{d+1})_{d+1} = 1$.

248 The optimal value of (3.15) gives a lower bound on the dual problem (3.10), and
 249 hence on the primal problem (3.9).

250 *Proof.* Based on the hyper-plane arrangements D_1, \dots, D_p , the dual constraint is
 251 equivalent to that for all $j \in [p]$,

$$252 \quad (3.16) \quad |2 \operatorname{tr}(D_j) \|w\|_2^2 - 2w^T \Lambda^T D_j X w| \leq \tilde{\beta}$$

253 holds for all $w \in \mathbb{R}^d$ satisfying $\|w\|_2 \leq 1, (2D_j - I)Xw \geq 0$. This is equivalent to say
 254 that for all $j \in [p]$

$$\begin{aligned} 255 \quad (3.17) \quad & \tilde{\beta} \geq \min 2 \operatorname{tr}(D_j) \|w\|_2^2 - 2w^T \Lambda^T D_j X w, \\ 256 & \text{s.t. } \|w\|_2 \leq 1, 2(D_j - I)Xw \geq 0, \\ 257 & -\tilde{\beta} \leq \max 2 \operatorname{tr}(D_j) \|w\|_2^2 - 2w^T \Lambda^T D_j X w, \\ 258 & \text{s.t. } \|w\|_2 \leq 1, 2(D_j - I)Xw \geq 0. \end{aligned}$$

260 From a convex optimization perspective, the natural idea to interpret the con-
 261 straint (3.17) is to transform the minimization problem into a maximization problem.
 262 We can rewrite the minimization problem in (3.17) as a trust region problem with
 263 inequality constraints:

$$\begin{aligned} 264 \quad (3.18) \quad & \min_{w \in \mathbb{R}^d} w^T (B_j + A_j(\Lambda)) w, \\ & \text{s.t. } \|w\|_2 \leq 1, (2D_j - I)Xw \geq 0. \end{aligned}$$

265 As the problem (3.18) is a convex problem, by taking the dual of (3.18) w.r.t. w ,
 266 we can transform (3.18) into a maximization problem. However, as (3.18) is a trust
 267 region problem with inequality constraints, the dual problem of (3.18) can be very
 268 complicated. According to [26], the optimal value of the problem (3.18) is bounded
 269 by the optimal value of the following SDP

$$\begin{aligned} 270 \quad (3.19) \quad & \min_{Z \in \mathbb{S}^{d+1}} \operatorname{tr}((\tilde{A}_j(\Lambda) + \tilde{B}_j)Z), \\ & \text{s.t. } \operatorname{tr}(H_n^{(j)} Z) \leq 0, n = 0, \dots, N, \\ & Z_{d+1, d+1} = 1, Z \succeq 0. \end{aligned}$$

271 from below.

272 LEMMA 3.6. *The dual problem of SDP (3.19) takes the form*

$$273 \quad (3.20) \quad \max -\gamma, \text{ s.t. } S = \tilde{A}_j(\Lambda) + \tilde{B}_j + \sum_{n=0}^N r_n H_n^{(j)} + \gamma e_{d+1} e_{d+1}^T, r \geq 0, S \succeq 0,$$

$$274 \quad \text{in variables } r = \begin{bmatrix} r_0 \\ \vdots \\ r_N \end{bmatrix} \in \mathbb{R}^{N+1} \text{ and } \gamma \in \mathbb{R}.$$

275 *Proof.* Consider the Lagrangian

$$276 \quad (3.21) \quad L(Z, r, \gamma) = \operatorname{tr}((\tilde{A}_j(\Lambda) + \tilde{B}_j)Z) + \sum_{n=0}^N r_n \operatorname{tr}(H_n^{(j)} Z) + \gamma(\operatorname{tr}(Z e_{d+1} e_{d+1}^T) - 1),$$

277 where $r \in \mathbb{R}_+^{N+1}$ and $\gamma \in \mathbb{R}$. By minimizing $L(Z, r, \gamma)$ w.r.t. $Z \in \mathbb{S}_+^{d+1}$, we derive the
 278 dual problem (3.20). \square

279 The constraints on Λ in the dual problem (3.10) include that the optimal value
 280 of (3.19) is bounded from below by $-\tilde{\beta}$. According to Lemma 3.6, this constraint is
 281 equivalent to that there exist $r \in \mathbb{R}^{N+1}$ and γ such that

$$282 \quad (3.22) \quad -\gamma \geq -\tilde{\beta}, S = \tilde{A}_j(\Lambda) + \tilde{B}_j + \sum_{n=0}^N r_n H_n^{(j)} + \gamma e_{d+1} e_{d+1}^T, r \geq 0, S \succeq 0.$$

283 As $e_{d+1} e_{d+1}^T$ is positive semi-definite, the above condition on Λ is also equivalent to
 284 that there exist $r \in \mathbb{R}^{N+1}$ such that

$$285 \quad (3.23) \quad \tilde{A}_j(\Lambda) + \tilde{B}_j + \sum_{n=0}^N r_n H_n^{(j)} + \tilde{\beta} e_{d+1} e_{d+1}^T \succeq 0, r \geq 0.$$

286 Therefore, the following convex set of Λ

$$287 \quad (3.24) \quad \left\{ \Lambda : \tilde{A}_j(\Lambda) + \tilde{B}_j + \sum_{n=0}^N r_n^{(j,-)} H_n^{(j)} + \tilde{\beta} e_{d+1} e_{d+1}^T \succeq 0, r^{(j,-)} \geq 0 \right\}$$

288 is a subset of the set of Λ satisfying the dual constraints

$$289 \quad (3.25) \quad \left\{ \Lambda : \min_{\|w\|_2 \leq 1, (2D_j - I)w \geq 0} w^T (B_j + A_j(\Lambda)) w \geq -\tilde{\beta} \right\}.$$

290 On the other hand, the constraint on Λ

$$291 \quad (3.26) \quad \max_{\|w\|_2 \leq 1, (2D_j - I)w \geq 0} w^T (B_j + A_j(\Lambda)) w \leq \tilde{\beta}$$

292 is equivalent to

$$293 \quad (3.27) \quad \min_{\|w\|_2 \leq 1, (2D_j - I)w \geq 0} -w^T (B_j + A_j(\Lambda)) w \geq -\tilde{\beta}.$$

294 By applying the previous analysis on the above trust region problem, the following
 295 convex set of Λ

$$296 \quad (3.28) \quad \left\{ \Lambda : -\tilde{A}_j(\Lambda) - \tilde{B}_j + \sum_{n=0}^N r_n^{(j,+)} H_n^{(j)} + \tilde{\beta} e_{d+1} e_{d+1}^T \succeq 0, r^{(j,+)} \geq 0 \right\}$$

297 is a subset of the set of Λ satisfying the dual constraints

$$298 \quad (3.29) \quad \left\{ \Lambda : \max_{\|w\|_2 \leq 1, (2D_j - I)w \geq 0} w^T (B_j + A_j(\Lambda)) w \leq \tilde{\beta} \right\}.$$

299 Therefore, replacing the dual constraint by

$$300 \quad (3.30) \quad \begin{aligned} & \tilde{A}_j(\Lambda) + \tilde{B}_j + \sum_{n=0}^N r_n^{(j,-)} H_n^{(j)} + \tilde{\beta} e_{d+1} e_{d+1}^T \succeq 0, j \in [p], \\ & -\tilde{A}_j(\Lambda) - \tilde{B}_j + \sum_{n=0}^N r_n^{(j,+)} H_n^{(j)} + \tilde{\beta} e_{d+1} e_{d+1}^T \succeq 0, j \in [p], \\ & r^{(j,-)} \geq 0, r^{(j,+)} \geq 0, j \in [p], \end{aligned}$$

301 we obtain the relaxed dual problem. As its feasible domain is a subset of the feasible
 302 domain of the dual problem, the optimal value of the relaxed dual problem gives a
 303 lower bound for the optimal value of the dual problem. \square

304 Now we consider the case when the relaxation is inexact, i.e., the relaxed dual
 305 problem has a smaller optimal value compared to the dual problem. In this case, the
 306 relaxed bi-dual problem provides insights on approximating the primal problem via
 307 convex optimization, which is derived as follows. As an equivalent formulation of the
 308 convex dual problem (3.15), it can be viewed as a convex relaxation of the primal
 309 problem (3.9).

310 PROPOSITION 3.7 (Relaxed bi-dual problem). *The dual of the relaxed dual prob-*
 311 *lem (3.15) is as follows*

$$\begin{aligned}
 & \min_{Z, \{(S^{(j,+)}, S^{(j,-)})\}_{j=1}^p} \frac{1}{2} \|Z + Y\|_F^2 - \frac{1}{2} \|Y\|_F^2 \\
 & + \sum_{j=1}^p \text{tr}(\tilde{B}_j(S^{(j,+)} - S^{(j,-)})) \\
 312 \quad (3.31) \quad & + \tilde{\beta} \sum_{j=1}^p \text{tr} \left((S^{(j,+)} + S^{(j,-)}) e_{d+1} e_{d+1}^T \right), \\
 & \text{s.t. } Z = \sum_{j=1}^p \tilde{A}_j^*(S^{(j,-)} - S^{(j,+)}), \\
 & \text{tr}(S^{(j,-)} H_n^{(j)}) \leq 0, \text{tr}(S^{(j,+)} H_n^{(j)}) \leq 0, \\
 & n = 0, \dots, N, j \in [p].
 \end{aligned}$$

313 Here A_j^* is the adjoint operator of the linear operator A_j .

314 *Proof.* Consider the Lagrangian function
 315 (3.32)

$$\begin{aligned}
 & L(\Lambda, \mathbf{r}, \mathbf{S}) \\
 & = -\frac{1}{2} \|\Lambda + Y\|_2^2 - \sum_{j=1}^p \text{tr} \left(S^{(j,-)} \left(\tilde{A}_j(\Lambda) + \tilde{B}_j + \sum_{n=0}^N r_n^{(j,-)} H_n^{(j)} + \frac{\tilde{\beta}}{2} e_{d+1} e_{d+1}^T \right) \right) \\
 315 \quad & - \sum_{j=1}^p \text{tr} \left(S^{(j,+)} \left(-\tilde{A}_j(\Lambda) - \tilde{B}_j + \sum_{n=0}^N r_n^{(j,+)} H_n^{(j)} + \frac{\tilde{\beta}}{2} e_{d+1} e_{d+1}^T \right) \right),
 \end{aligned}$$

316 where we write

$$\begin{aligned}
 317 \quad (3.33) \quad & \mathbf{r} = (r^{(1,-)}, \dots, r^{(p,-)}, r^{(1,+)}, \dots, r^{(p,+)}) \in (\mathbb{R}^{N+1})^{2p}, \\
 & \mathbf{S} = (S^{(1,-)}, \dots, S^{(p,-)}, S^{(1,+)}, \dots, S^{(p,+)}) \in (\mathbb{S}_+^{d+1})^{2p}.
 \end{aligned}$$

318 Here we write $\mathbb{S}_+^{d+1} = \{S \in \mathbb{S}^{d+1} | S \succeq 0\}$. By maximizing w.r.t. Λ and \mathbf{r} , we derive
 319 the bi-dual problem (3.31). \square

320 As (3.15) is a convex problem and the Slater's condition is satisfied, the optimal values
 321 of (3.15) and (3.31) are same. The bi-dual problem (3.31) is closely related to the
 322 primal problem (3.9). Indeed, any feasible solutions of the primal problem (3.5) can
 323 be mapped to feasible solutions of (3.31). We note that the mapping from the primal
 324 solution to the bi-dual solution cannot go both ways unless these two problems are
 325 equivalent.

326 **THEOREM 3.8.** *Suppose that (Z, W, α) is feasible to the primal problem (3.9).
 327 Then, there exist matrices $\{S^{(j,+)}, S^{(j,-)}\}_{j=1}^p$ constructed from (W, α) such that
 328 $(Z, \{S^{(j,+)}, S^{(j,-)}\}_{j=1}^p)$ is feasible to the relaxed bi-dual problem (3.31). Moreover,
 329 the objective value of the relaxed bi-dual problem (3.31) at $(Z, \{S^{(j,+)}, S^{(j,-)}\}_{j=1}^p)$ is
 330 the same as objective value of the primal problem (3.9) at (Z, W, α) .*

331 *Proof.* Suppose that (Z, W, α) is a feasible solution to (3.5). Let D_{j_1}, \dots, D_{j_k} be
 332 the enumeration of $\{\mathbf{diag}(\mathbb{I}(Xw_i \geq 0)) \mid i \in [m]\}$. For $i \in [k]$, we let

$$333 \quad (3.34) \quad S^{(j_i,+)} = \sum_{l:\alpha_l \geq 0, \mathbf{diag}(\mathbb{I}(Xw_l \geq 0))=D_{j_i}} \alpha_l \begin{bmatrix} w_l w_l^T & w_l \\ w_l^T & 1 \end{bmatrix}, S^{(j_i,-)} = 0,$$

334 and

$$335 \quad (3.35) \quad S^{(j_i,+)} = 0, S^{(j_i,-)} = - \sum_{l:\alpha_l < 0, \mathbf{diag}(\mathbb{I}(Xw_l \geq 0))=D_{j_i}} \alpha_l \begin{bmatrix} w_l w_l^T & w_l \\ w_l^T & 1 \end{bmatrix}.$$

336 For $j \notin \{j_1, \dots, j_k\}$, we simply set $S^{(j,+)} = 0, S^{(j,-)} = 0$. As $\|w_i\|_2 \leq 1$ and $D_{j_i} =$
 337 $\mathbb{I}(Xw_i \geq 0)$, we can verify that $\text{tr}(S^{(j,-)} H_n^{(j)}) \leq 0, \text{tr}(S^{(j,+)} H_n^{(j)}) \leq 0$ are satisfied for
 338 $j = j_1, \dots, j_m$ and $n = 0, 1, \dots, N$. This is because for $n = 0$, as $H_0^{(j_i)} = \begin{bmatrix} I_d & 0 \\ 0 & -1 \end{bmatrix}$,
 339 it follows that

$$340 \quad (3.36) \quad \begin{aligned} \text{tr}(S^{(j_i,+)} H_0^{(j_i)}) &= \sum_{l:\alpha_l \geq 0, \mathbf{diag}(\mathbb{I}(Xw_l \geq 0))=D_{j_i}} \alpha_l (\|w_l\|^2 - 1) \leq 0, \\ \text{tr}(S^{(j_i,-)} H_0^{(j_i)}) &= - \sum_{l:\alpha_l < 0, \mathbf{diag}(\mathbb{I}(Xw_l \geq 0))=D_{j_i}} \alpha_l (\|w_l\|^2 - 1) \leq 0. \end{aligned}$$

341 For $n = 1, \dots, N$, we have

$$342 \quad (3.37) \quad \begin{aligned} \text{tr}(S^{(j_i,+)} H_0^{(j_i)}) &= \sum_{l:\alpha_l \geq 0, \mathbf{diag}(\mathbb{I}(Xw_l \geq 0))=D_{j_i}} 2\alpha_l (1 - 2(D_{j_i})_{nn}) x_n^T w_l \leq 0, \\ \text{tr}(S^{(j_i,-)} H_0^{(j_i)}) &= - \sum_{l:\alpha_l < 0, \mathbf{diag}(\mathbb{I}(Xw_l \geq 0))=D_{j_i}} \alpha_l (1 - 2(D_{j_i})_{nn}) x_n^T w_l \leq 0. \end{aligned}$$

343 Based on the above transformation, we can rewrite the bidual problem in the
 344 form of the primal problem (3.9). For $S \in \mathbb{S}^{d+1}$, we note that

$$345 \quad \begin{aligned} &\text{tr}(S \tilde{A}_j(\Lambda)) \\ &= - \text{tr}((\Lambda^T D_j X + X^T D_j \Lambda) S_{1:d,1:d}) \\ &= - 2 \text{tr}(\Lambda^T D_j X S_{1:d,1:d}), \end{aligned}$$

where $S_{1:d,1:d}$ denotes the $d \times d$ block of S consisting the first d rows and columns.
 This implies that $\tilde{A}_j^*(S) = -2D_j X S_{1:d,1:d}$. Hence, we have

$$\begin{aligned} \tilde{A}_{j_i}(S^{(j_i,+)} - S^{(j_i,-)}) &= - \sum_{l:\mathbf{diag}(\mathbb{I}(Xw_l \geq 0))=D_{j_i}} 2\alpha_l D_{j_i} X w_l w_l^T \\ &= - \sum_{l:\mathbf{diag}(\mathbb{I}(Xw_l \geq 0))=D_{j_i}} 2\alpha_l (Xw_l)_+ w_l^T. \end{aligned}$$

Therefore, we have

$$\sum_{j=1}^p \tilde{A}_j^*(S^{(j,-)} - S^{(j,+)}) = 2 \sum_{i=1}^m \alpha_i (Xw_i)_+ w_i^T.$$

As n -th row of Z satisfies that $z_n = 2 \sum_{i=1}^m \alpha_i w_i (x_n^T w_i)_+$, this implies that

$$Z = 2 \sum_{i=1}^m \alpha_i (Xw_i)_+ w_i^T = \sum_{j=1}^p \tilde{A}_j^*(S^{(j,-)} - S^{(j,+)}).$$

346 Hence $(Z, \{(S^{(j,-)}, S^{(j,-)})_{j=1}^p\})$ is feasible to the relaxed bi-dual problem (3.31).

We can also compute that

$$\sum_{j=1}^p \text{tr}(\tilde{B}_j(S^{(j,+)} - S^{(j,-)})) = 2 \sum_{i=1}^m \alpha_i \sum_{n=1}^N \mathbb{I}(x_n^T w_i \geq 0) \|w_i\|_2^2,$$

and

$$\sum_{j=1}^p \text{tr}((S^{(j,+)} + S^{(j,-)})e_{d+1}e_{d+1}^T) = \sum_{i=1}^m |\alpha_i|.$$

347 Thus, the primal problem (3.9) with (Z, W, α) and the relaxed bi-dual problem (3.31)
348 with $(Z, \{(S^{(j,-)}, S^{(j,-)})_{j=1}^p\})$ have the same objective value. \square

349 Let $J(Z, \{S^{(j,+)}, S^{(j,-)}\}_{j=1}^p)$ denote the objective value of the relaxed bi-dual prob-
350 lem (3.31) at a feasible solution $(Z, \{S^{(j,+)}, S^{(j,-)}\}_{j=1}^p)$. Let (Z^*, W^*, α^*) denote a
351 globally optimal solution of the primal problem (3.9). By Theorem 3.8, there exist
352 matrices $\{S^{(j,+)}, S^{(j,-)}\}_{j=1}^p$ such that $(Z^*, \{S^{(j,+)}, S^{(j,-)}\}_{j=1}^p)$ is a feasible solution of
353 the relaxed bi-dual problem (3.31) and $J(Z^*, \{S^{(j,+)}, S^{(j,-)}\}_{j=1}^p)$ is the same as the
354 objective value of (3.9) at its global minimum (Z^*, W^*, α^*) . On the other hand, let
355 $(\tilde{Z}^*, \{\tilde{S}^{(j,+)}, \tilde{S}^{(j,-)}\}_{j=1}^p)$ denote an optimal solution of the relaxed bi-dual problem
356 (3.31). From the optimality of $(\tilde{Z}^*, \{\tilde{S}^{(j,+)}, \tilde{S}^{(j,-)}\}_{j=1}^p)$, we have

$$357 \quad J(\tilde{Z}^*, \{\tilde{S}^{(j,+)}, \tilde{S}^{(j,-)}\}_{j=1}^p) \leq J(Z^*, \{S^{(j,+)}, S^{(j,-)}\}_{j=1}^p).$$

358 Note that at (Z^*, W^*, α^*) we obtain the optimal approximation of $\nabla \log \rho - \nabla \log \pi$ at
359 x_1, \dots, x_N in the family of two-layer squared-ReLU networks (3.1). Smaller or equal
360 objective value of the relaxed bi-dual problem (3.31) can be achieved at the pair
361 $(\tilde{Z}^*, \{\tilde{S}^{(j,+)}, \tilde{S}^{(j,-)}\}_{j=1}^p)$ than at $(Z^*, \{S^{(j,+)}, S^{(j,-)}\}_{j=1}^p)$. Therefore, we can view \tilde{Z}^*
362 gives an optimal approximation of $\nabla \log \rho - \nabla \log \pi$ evaluated on x_1, \dots, x_N in a
363 broader function family including the two-layer squared ReLU neural networks.

364 From the derivation of the relaxed bi-dual problem, we have the relation $\tilde{Z}^* =$
365 $-\Lambda^* - Y$, where $(\Lambda^*, \{r^{(j,+)}, r^{(j,-)}\})$ is optimal to the relaxed dual problem (3.15) and
366 $(\tilde{Z}^*, \{\tilde{S}^{(j,+)}, \tilde{S}^{(j,-)}\}_{j=1}^p)$ is optimal to the relaxed bi-dual problem (3.31). Therefore,
367 by solving Λ^* from the relaxed dual problem (3.15), we can use $-\Lambda^* - Y$ as the
368 approximation of $\nabla \log \rho - \nabla \log \pi$ evaluated on x_1, \dots, x_N .

369 *Remark 3.9.* We note that solving the proposed convex optimization problem
370 3.15 renders the approximation of the Wasserstein gradient direction. Compared to
371 the two-layer ReLU networks, it induces a broader class of functions represented by
372 $\{S^{(j,+)}, S^{(j,-)}\}_{j=1}^p$. This contains more variables than the neural network function.

373 **3.2. Choice of the regularization parameter.** As the constraints in the re-
 374 laxd dual problem (3.15) depend on the regularization parameter $\tilde{\beta}$, it is possible
 375 that for small $\tilde{\beta}$, the relaxed dual problem (3.15) is infeasible. Consider the following
 376 SDP

$$\begin{aligned}
 & \min \tilde{\beta}, \text{ s.t. } \tilde{A}_j(\Lambda) + \tilde{B}_j + \sum_{n=0}^N r_n^{(j,-)} H_n^{(j)} + \tilde{\beta} e_{d+1} e_{d+1}^T \succeq 0, \\
 & -\tilde{A}_j(\Lambda) - \tilde{B}_j + \sum_{n=0}^N r_n^{(j,+)} H_n^{(j)} + \tilde{\beta} e_{d+1} e_{d+1}^T \succeq 0, \\
 & r^{(j,-)} \geq 0, r^{(j,+)} \geq 0, j \in [p].
 \end{aligned}
 \tag{3.38}$$

378 Here the variables are $\tilde{\beta}, \Lambda$ and $\{r^{(j,+)}, r^{(j,-)}\}_{j=1}^p$. Let $\tilde{\beta}_1$ be the optimal value of
 379 the above problem. Then, only for $\tilde{\beta} \geq \tilde{\beta}_1$, there exists $\Lambda \in \mathbb{R}^{N \times d}$ satisfying the
 380 constraints in (3.15). In other words, the relaxed dual problem (3.15) is feasible. We
 381 also note that $\tilde{\beta}_1$ only depends on the samples X and it does not depend on the value
 382 of $\nabla \log \pi$ evaluated on x_1, \dots, x_N . On the other hand, consider the following SDP

$$\begin{aligned}
 & \min \tilde{\beta}, \text{ s.t. } \tilde{A}_j(Y) + \tilde{B}_j + \sum_{n=0}^N r_n^{(j,-)} H_n^{(j)} + \tilde{\beta} e_{d+1} e_{d+1}^T \succeq 0, \\
 & -\tilde{A}_j(Y) - \tilde{B}_j + \sum_{n=0}^N r_n^{(j,+)} H_n^{(j)} + \tilde{\beta} e_{d+1} e_{d+1}^T \succeq 0, \\
 & r^{(j,-)} \geq 0, r^{(j,+)} \geq 0, j \in [p],
 \end{aligned}
 \tag{3.39}$$

384 where the variables are $\tilde{\beta}$ and $\{r^{(j,+)}, r^{(j,-)}\}_{j=1}^p$. Let $\tilde{\beta}_2$ be the optimal value of the
 385 above problem. For $\tilde{\beta} \geq \tilde{\beta}_2$, as Y is feasible for the constraints in (3.15), the optimal
 386 value of the relaxed dual problem (3.15) is 0. In short, only when $\tilde{\beta} \in [\tilde{\beta}_1, \tilde{\beta}_2]$, the
 387 variational problem (3.15) is non-trivial. To ensure that solving the relaxed dual
 388 problem (3.15) gives a good approximation of the Wasserstein gradient direction, we
 389 shall avoid choosing $\tilde{\beta}$ either too small or too large.

390 **3.3. Practical implementation.** Although the number p of all possible hyper-
 391 plane arrangements is upper bounded by $2r((N-1)e/r)^r$ with $r = \text{rank}(X)$, it is
 392 computationally costly to enumerate all possible p matrices D_1, \dots, D_p to represent
 393 the constraints in the relaxed dual problem (3.5). In practice, we first randomly
 394 sample M i.i.d. random vectors $u_1, \dots, u_M \sim \mathcal{N}(0, I_d)$ and generate a subset $\hat{\mathcal{S}} =$
 395 $\{\text{diag}(\mathbb{I}(Xu_j \geq 0)) | j \in [M]\}$. of \mathcal{S} . Then, we optimize the randomly sub-sampled
 396 version of the relaxed dual problem based on the subset $\hat{\mathcal{S}}$ and obtain the solution
 397 Λ . Here $-\Lambda - Y$ is used as the direction to update the particle system X . If the
 398 regularization parameter is too large, then we will have $-\Lambda - Y = 0$, which makes the
 399 particle system unchanged. Therefore, to ensure that $\tilde{\beta}$ is not too large, we decay $\tilde{\beta}$
 400 by a factor $\gamma_1 \in (0, 1)$. This also appears in [19]. On the other hand, if $\tilde{\beta}$ is too small
 401 resulting the relaxed dual problem (3.5) infeasible, we increase $\tilde{\beta}$ by multiplying γ_2^{-1} ,
 402 where $\gamma_2 \in (0, 1)$. The overall algorithm is summarized in Algorithm 3.1.

403 Applying the standard interior point method [7] leads to the computational time

$$\tag{3.40} \quad O((\max\{N, d^2\} \hat{p})^6).$$

405 For high-dimensional problems, i.e., d is large, the computational cost of solving (3.15)
 406 can be large. In this case, we apply the dimension-reduction techniques [55, 11, 48] to

Algorithm 3.1 Convex neural Wasserstein descent

Require: initial positions $\{x_0^n\}_{n=1}^N$, step size α_l , initial regularization parameter $\tilde{\beta}_0$, $\gamma_1, \gamma_2 \in (0, 1)$.

- 1: **while** not converge **do**
- 2: Form X_l and Y_l based on $\{x_l^n\}_{n=1}^N$ and $\{\nabla \log \pi(x_l^n)\}_{n=1}^N$.
- 3: Solve Λ_l from the relaxed dual problem (3.15) with $\tilde{\beta} = \tilde{\beta}_l$.
- 4: **if** the relaxed dual problem with $\tilde{\beta} = \tilde{\beta}_l$ is infeasible **then**
- 5: Set $X_{l+1} = X_l$ for $n \in [N]$ and set $\tilde{\beta}_{l+1} = \gamma_2^{-1} \tilde{\beta}_l$.
- 6: **else**
- 7: Update $X_{l+1} = X_l + \alpha_l(\Lambda_l + Y_l)$ for $n \in [N]$ and set $\tilde{\beta}_{l+1} = \gamma_1 \tilde{\beta}_l$.
- 8: **end if**
- 9: **end while**

407 reduce the parameter dimension d to a data-informed intrinsic dimension \hat{d} , which is
 408 often very low, i.e., $\hat{d} \ll d$, thus significantly reducing the computational time (3.40).

409 **4. Numerical experiments.** In this section, we present numerical results to
 410 compare WGD approximated by neural networks (WGD-NN) and WGD approx-
 411 imated using convex optimization formulation of neural networks (WGD-cvxNN).
 412 The performance of compared methods is assessed by the sample goodness-of-fit of
 413 the posterior. For WGD-NN, in each iteration, it updates the particle system using
 414 (2.3) with a function Φ represented by a two-layer squared ReLU neural network.
 415 The parameters of the neural network are obtained by directly solving the nonconvex
 416 optimization problem (3.4). For high-dimensional problems, we apply the dimension
 417 reduction technique and compare the projected versions (pWGD-NN and pWGD-
 418 cvxNN).

419 We note that although the cost for solving the relaxed dual problem (3.15) using
 420 standard convex optimization solvers in WGD-cvxNN can be higher compared to that
 421 by a direct neural network training in WGD-NN, this cost difference is negligible in
 422 the entire optimization dominated by the likelihood evaluation when the model (e.g.,
 423 PDE) is expensive to solve. In such cases, WGD-cvxNN and WGD-NN have similar
 424 computational complexity but WGD-cvxNN achieves better performance. We use
 425 the standard convex optimization solver CVXPY [16] with MOSEK[3] inner solver.
 426 Applying randomized SDP solvers [54], randomized second-order methods [43, 31] or
 427 advanced SDP solvers [56, 53, 49] for the large-scale problem can improve the com-
 428 putation time. Moreover, the induced SDPs have specific structures of many similar
 429 constraints. Solving the SDP (3.15) can be accelerated by designing a specialized
 430 convex optimization solver, which is left for future work.

431 **4.1. A two-dimensional example.** We test and compare the performance of
 432 WGD-cvxNN and WGD-NN on a bimodal two-dimensional double-banana posterior
 433 distribution introduced in [14]. We first generate 300 posterior samples by a Stein
 434 variational Newton (SVN) method [14] as the reference, as shown in Figure 1. We
 435 evaluate the performance of WGD-NN and WGD-cvxNN by calculating the maximum
 436 mean discrepancy (MMD) between their samples in each iteration and the reference
 437 samples. In the comparison, we use $N = 50$ samples and run for 100 iterations with
 438 step sizes $\alpha_l = 10^{-3}$. For WGD-cvxNN, we set $\beta = 1$, $\gamma_1 = 0.95$ and $\gamma_2 = 0.95^{10}$. For
 439 WGD-NN, we use $m = 200$ neurons and optimize the regularized training problem
 440 (3.4) using all samples with the Adam optimizer [29] with learning rate 10^{-3} for 200

441 sub-iterations. We also set the regularization parameter $\beta = 1$ and decrease it by a
 442 factor of 0.95 in each iteration. We find that this setup of parameters is more suitable.

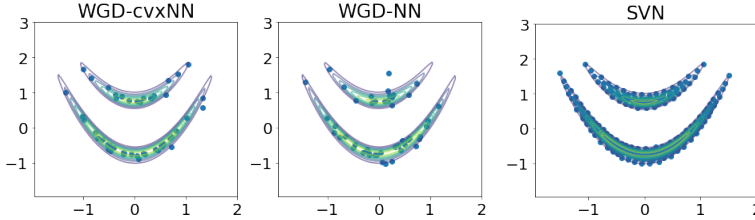


Fig. 1: Two-dimensional example. Posterior density and sample distributions by WGD-cvxNN and WGD-NN at the final step of 100 iterations, compared to the reference SVN samples (right).

443 The posterior density and the sample distributions by WGD-cvxNN and WGD-
 444 NN at the final step of 100 iterations are shown in Figure 1. It can be observed that
 445 WGD-cvxNN provides more representative samples than WGD-NN for the posterior
 446 density. In Figure 2, we plot the MMD of the samples by WGD-cvxNN and WGD-NN
 447 compared to the reference SVN samples at each iteration. We observe that the samples
 448 by WGD-cvxNN achieve much smaller MMD than those of WGD-NN compared to
 449 the reference SVN samples, which is consistent with the results shown in Figure 1.

4.2. PDE-constrained linear Bayesian inference. In this experiment, we consider a linear Bayesian inference problem constrained by a partial differential equation (PDE) model for contaminant diffusion in environmental engineering in the domain $D = (0, 1)$,

$$-\kappa\Delta u + \nu u = \xi \quad \text{in } D,$$

450 where ξ is a contaminant source field parameter in domain D , u is the contaminant
 451 concentration which we can observe at some locations, κ and ν are diffusion and
 452 reaction coefficients. For simplicity, we set $\kappa, \nu = 1$, $u(0) = u(1) = 0$, and consider 15
 453 pointwise observations of u with 1% noise, equidistantly distributed in D . We consider
 454 a Gaussian prior distribution $\xi \sim \mathcal{N}(0, C)$ with covariance given by a differential
 455 operator $C = (-\delta\Delta + \gamma I)^{-\alpha}$ with $\delta, \gamma, \alpha > 0$ representing the correlation length
 456 and variance, which is commonly used in geoscience. We set $\delta = 0.1, \gamma = 1, \alpha = 1$.
 457 In this linear setting, the posterior is Gaussian with the mean and covariance given
 458 analytically, which are used as a reference to assess the sample goodness. We solve
 459 this forward model by a finite element method with piece-wise linear elements on a
 460 uniform mesh of size 2^k , $k \geq 1$. We project this high-dimensional parameter to the
 461 data-informed low dimensions as in [48] to alleviate the curse of dimensionality when
 462 applying WGD-cvxNN and WGD-NN, which we call pWGD-cvxNN and pWGD-NN,
 463 respectively. For $k = 4$ we have 17 dimensions for the discrete parameter and 4
 464 dimensions after projection.

465 We run pWGD-cvxNN and pWGD-NN using 16 samples for 200 iterations with
 466 $\alpha_l = 10^{-3}$, $\beta = 5$, $\gamma_1 = 0.95$, and $\gamma_2 = 0.95^{10}$ for both methods. We use $m = 200$
 467 neurons for pWGD-NN and train it by the Adam optimizer for 200 sub-iterations as
 468 in the first example. From Figure 3, we observe that pWGD-cvxNN achieves better
 469 root mean squared error (RMSE) than pWGD-NN for both the sample mean and the
 470 sample variance compared to the reference.

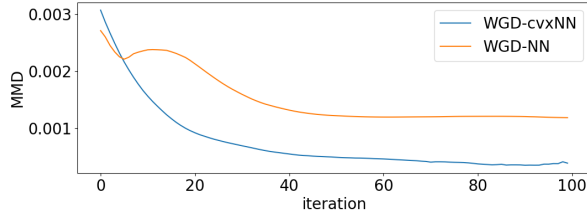


Fig. 2: Two-dimensional example. Maximum mean discrepancy (MMD) of WGD-cvxNN and WGD-NN samples compared to the reference SVN samples.

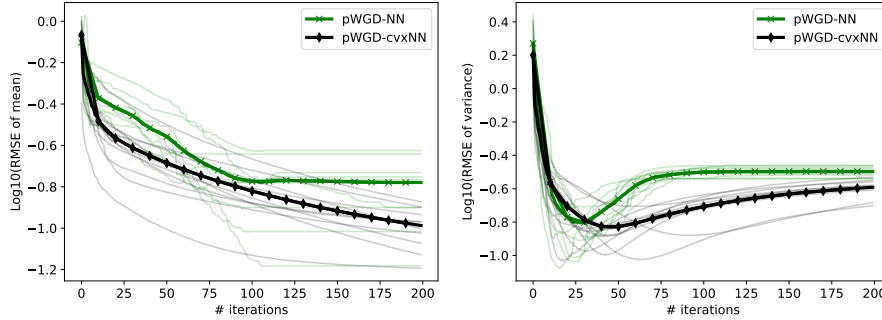


Fig. 3: PDE-constrained linear Bayesian inference. Ten trials and the RMSE of the sample mean (top) and sample variance (bottom) by pWGD-NN and pWGD-cvxNN at different iterations.

471 **4.3. PDE-constrained nonlinear Bayesian inference.** In this experiment,
 472 we consider a nonlinear Bayesian inference problem constrained by the following partial
 473 differential equation (PDE) [11] with application to subsurface (Darcy) flow in a
 474 physical domain $D = (0, 1)^2$,

$$475 \quad (4.1) \quad \begin{aligned} \mathbf{v} + e^\xi \nabla u &= 0 && \text{in } D, \\ \nabla \cdot \mathbf{v} &= h && \text{in } D, \end{aligned}$$

476 where u is pressure, \mathbf{v} is velocity, h is force, e^ξ is a random (permeability) field
 477 equipped with a Gaussian prior $\xi \sim \mathcal{N}(\xi_0, C)$ with covariance operator $C = (-\delta\Delta +$
 478 $\gamma I)^{-\alpha}$ where we set $\delta = 0.1, \gamma = 1, \alpha = 2$ and $\xi_0 = 0$. This problem is widely
 479 used in many areas, for instance, in estimating permeability in groundwater flow,
 480 thermal conductivity in material science, or electrical impedance in medical imaging,
 481 We impose Dirichlet boundary conditions $u = 1$ on the top boundary and $u = 0$ on
 482 the bottom boundary, and homogeneous Neumann boundary conditions on the left
 483 and right boundaries for u . We use a finite element method with piecewise linear
 484 elements for the discretization of the problem, resulting in 81 dimensions for the
 485 discrete parameter. The data is generated as pointwise observation of the pressure
 486 field at 49 points equidistantly distributed in $(0, 1)^2$, corrupted with additive 5%
 487 Gaussian noise. We use a DILI-MCMC algorithm [13] with 10000 effective samples
 488 to compute the sample mean and sample variance, which are used as the reference
 489 values to assess the goodness of the samples.

490 We run pWGD-cvxNN and pWGD-NN with 64 samples for ten trials with step
 491 size $\alpha_l = 10^{-3}$, where we set $\beta = 10, \gamma_1 = 0.95$, and $\gamma_2 = 0.95^{10}$ for both methods.
 492 The RMSE of the sample mean and sample variance are shown in Figure 4 for the

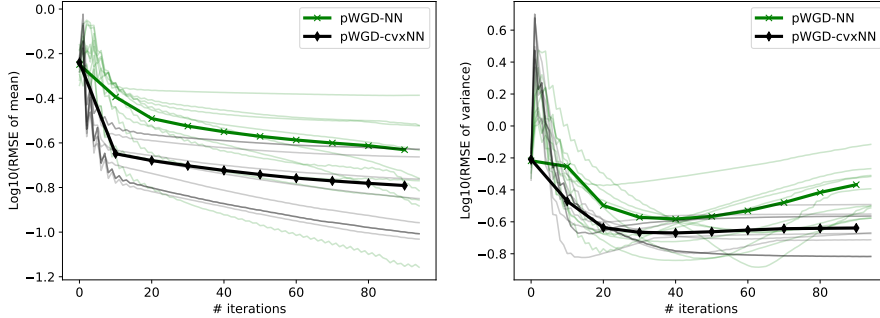


Fig. 4: PDE-constrained non-linear Bayesian inference. Ten trials and the RMSE of the sample mean (top) and sample variance (bottom) by pWGD-NN and pWGD-cvxNN at different iterations.

493 two methods at each of the iterations. We can observe that pWGD-cvxNN achieves
 494 smaller errors for both the sample mean and the sample variance compared to pWGD-
 495 NN at each iteration. Moreover, pWGD-cvxNN provides a much smaller variation of
 496 the sample mean and sample variance for the ten trials compared to pWGD-NN.
 497 Furthermore, by an effective reduction of the parameter dimension from 81 to data-
 498 informed 20 in our pWGD-cvxNN, as used and analyzed in [55, 11, 48], the time for
 499 solving the SDP is significantly reduced from about 800 seconds to about 0.7 seconds
 500 in average, making our pWGD-cvxNN computationally efficient.

501 **4.4. Bayesian inference for COVID-19.** In this experiment, we use Bayesian
 502 inference to learn the dynamics of the transmission and severity of COVID-19 from
 503 the recorded data for New York state. We use the model, parameter, and data as
 504 in [11]. More specifically, we use a compartmental model for the modeling of the
 505 transmission and outcome of COVID-19. We take the number of hospitalized cases as
 506 the observation data to infer a social distancing parameter, a time-dependent stochastic
 507 process that is equipped with a Tanh-Gaussian prior to model the transmission
 508 reduction effect of social distancing, which becomes 96 dimensions after discretization.

509 We use the projected Stein variational gradient descent (pSVGd) method [11]
 510 as the reference to evaluate the goodness of samples. We run pWGD-cvxNN and
 511 pWGD-NN using 64 samples for 100 iterations with step size $\alpha_l = 10^{-3}$, where we set
 512 $\beta = 10$, $\gamma_1 = 0.95$, and $\gamma_2 = 0.95^{10}$ for both methods as in the last example. From
 513 Figure 5 we can observe that pWGD-cvxNN produces more consistent results than
 514 pWGD-NN compared to the reference pSVGd results, for both the sample mean and
 515 90% credible interval, both in the inference of the social distancing parameter and in
 516 the prediction of the hospitalized cases.

517 **5. Conclusion.** In the context of Bayesian inference, we approximate the Wass-
 518 erstein gradient direction by the gradient of functions in the family of two-layer neural
 519 networks. We propose a convex SDP relaxation of the dual of the variational primal
 520 problem, which can be solved efficiently using convex optimization methods instead
 521 of directly training the neural network as a nonconvex optimization problem. In
 522 particular, we established that the gradient obtained by the new formulation and
 523 convex optimization is at least as good as the one approximated by functions in
 524 the family of two-layer neural networks, which is demonstrated by various numerical
 525 experiments. By stacking the two-layer neural networks in each step together, our

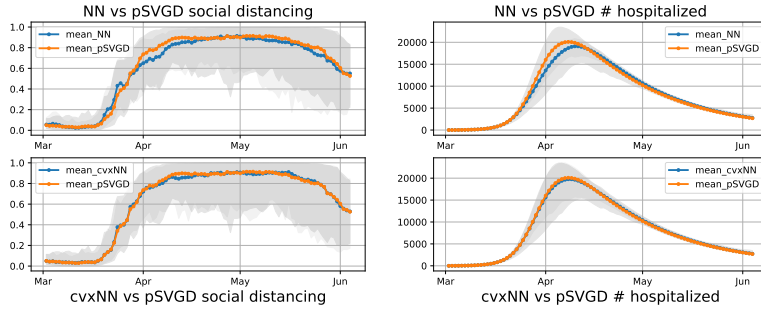


Fig. 5: Bayesian inference for COVID-19. Comparison of pWGD-cvxNN and pWGD-NN to the reference by pSVGD for Bayesian inference of the social distancing parameter (left) from the data of the hospitalized cases (right) with sample mean and 90% credible interval.

526 proposed method formulates a deep neural network to learn the transportation map
 527 from the prior to the posterior. In future studies, specialized optimization solvers
 528 for the structured SDPs, including the relaxed dual problem, can lead to significant
 529 accelerations of our proposed method. We also expect to apply deep neural networks
 530 for the approximation of Wasserstein gradient flows based on recent works on convex
 531 optimization formulations of deep neural networks [50, 17, 18]. Detailed study of the
 532 conditions where the SDP relaxation is tight is of great interest as it provides more
 533 insight from the convex optimization perspective to understand how neural networks
 534 fit the data and which kind of datasets is easier to learn. We also expect to bound
 535 the number of hyperplane arrangements needed for an approximate solution and give
 536 a useful guarantee that bounds the distance between solutions to perturbations of the
 537 convex problem in future research.

538

REFERENCES

- 539 [1] D. ALVAREZ-MELIS, Y. SCHIFF, AND Y. MROUEH, *Optimizing functionals on the space of prob-*
 540 *abilities with input convex neural networks*, arXiv preprint arXiv:2106.00774, (2021).
 541 [2] L. AMBROSIO, N. GIGLI, AND G. SAVARÉ, *Gradient flows: in metric spaces and in the space of*
 542 *probability measures*, Springer Science & Business Media, 2005.
 543 [3] M. APS, *Mosek optimization suite*, 2019.
 544 [4] B. BARTAN AND M. PILANCI, *Neural spectrahedra and semidefinite lifts: Global convex opti-*
 545 *mization of polynomial activation neural networks in fully polynomial-time*, arXiv preprint
 546 arXiv:2101.02429, (2021).
 547 [5] B. BARTAN AND M. PILANCI, *Training quantized neural networks to global optimality via semi-*
 548 *definite programming*, in International Conference on Machine Learning, PMLR, 2021,
 549 pp. 694–704.
 550 [6] C. BONET, N. COURTY, F. SEPTIER, AND L. DRUMETZ, *Sliced-wasserstein gradient flows*, arXiv
 551 preprint arXiv:2110.10972, (2021).
 552 [7] S. BOYD, S. P. BOYD, AND L. VANDENBERGHE, *Convex optimization*, Cambridge university
 553 press, 2004.
 554 [8] C. BUNNE, L. MENG-PAPAXANTHOS, A. KRAUSE, AND M. CUTURI, *Jkonet: Proximal optimal*
 555 *transport modeling of population dynamics*, arXiv preprint arXiv:2106.06345, (2021).
 556 [9] J. A. CARRILLO, K. CRAIG, L. WANG, AND C. WEI, *Primal dual methods for wasserstein*
 557 *gradient flows*, Foundations of Computational Mathematics, (2021), pp. 1–55.
 558 [10] J. A. CARRILLO, D. MATTHES, AND M.-T. WOLFRAM, *Lagrangian schemes for wasserstein*
 559 *gradient flows*, Handbook of Numerical Analysis, 22 (2021), pp. 271–311.
 560 [11] P. CHEN AND O. GHATTAS, *Projected stein variational gradient descent*, Advances in Neural
 561 Information Processing Systems, 33 (2020), pp. 1947–1958.
 562 [12] T. M. COVER, *Geometrical and statistical properties of systems of linear inequalities with*

- 563 *applications in pattern recognition*, IEEE transactions on electronic computers, (1965),
564 pp. 326–334.
- [13] T. CUI, K. J. LAW, AND Y. M. MARZOUK, *Dimension-independent likelihood-informed mcmc*,
565 Journal of Computational Physics, 304 (2016), pp. 109–137.
- [14] G. DETOMMASO, T. CUI, A. SPANTINI, Y. MARZOUK, AND R. SCHEICHL, *A stein variational*
566 *newton method*, arXiv preprint arXiv:1806.03085, (2018).
- [15] L. L. DI LANGOSCO, V. FORTUIN, AND H. STRATHMANN, *Neural variational gradient descent*,
567 arXiv preprint arXiv:2107.10731, (2021).
- [16] S. DIAMOND AND S. BOYD, *CVXPY: A Python-embedded modeling language for convex opti-*
572 *mization*, Journal of Machine Learning Research, 17 (2016), pp. 1–5.
- [17] T. ERGEN AND M. PILANCI, *Global optimality beyond two layers: Training deep relu net-*
573 *works via convex programs*, in International Conference on Machine Learning, PMLR,
574 2021, pp. 2993–3003.
- [18] T. ERGEN AND M. PILANCI, *Path regularization: A convexity and sparsity inducing regulariza-*
576 *tion for parallel relu networks*, arXiv preprint arXiv:2110.09548, (2021).
- [19] T. ERGEN, A. SAHINER, B. OZTURKLER, J. PAULY, M. MARDANI, AND M. PILANCI, *Demystifying*
578 *batch normalization in relu networks: Equivalent convex optimization models and implicit*
579 *regularization*, arXiv preprint arXiv:2103.01499, (2021).
- [20] J. FAN, A. TAGHVAEI, AND Y. CHEN, *Variational wasserstein gradient flow*, arXiv preprint
581 arXiv:2112.02424, (2021).
- [21] X. FENG, Y. GAO, J. HUANG, Y. JIAO, AND X. LIU, *Relative entropy gradient sampler for*
583 *unnormalized distributions*, arXiv preprint arXiv:2110.02787, (2021).
- [22] C. FROGNER AND T. POGGIO, *Approximate inference with wasserstein gradient flows*, in Inter-
584 national Conference on Artificial Intelligence and Statistics, PMLR, 2020, pp. 2581–2590.
- [23] K. HORNIK, M. STINCHCOMBE, AND H. WHITE, *Multilayer feedforward networks are universal*
585 *approximators*, Neural networks, 2 (1989), pp. 359–366.
- [24] H. J. HWANG, C. KIM, M. S. PARK, AND H. SON, *The deep minimizing movement scheme*,
586 arXiv preprint arXiv:2109.14851, (2021).
- [25] A. HYVÄRINEN AND P. DAYAN, *Estimation of non-normalized statistical models by score match-*
587 *ing.*, Journal of Machine Learning Research, 6 (2005).
- [26] V. JEYAKUMAR AND G. LI, *Trust-region problems with linear inequality constraints: exact sdp*
589 *relaxation, global optimality and robust optimization*, Mathematical Programming, 147
590 (2014), pp. 171–206.
- [27] R. JORDAN, D. KINDERLEHRER, AND F. OTTO, *The variational formulation of the fokker–planck*
591 *equation*, SIAM journal on mathematical analysis, 29 (1998), pp. 1–17.
- [28] O. JUNGE, D. MATTHES, AND H. OSBERGER, *A fully discrete variational scheme for solving*
592 *nonlinear fokker–planck equations in multiple space dimensions*, SIAM Journal on Numerical
593 Analysis, 55 (2017), pp. 419–443.
- [29] D. P. KINGMA AND J. BA, *Adam: A method for stochastic optimization*, arXiv preprint
594 arXiv:1412.6980, (2014).
- [30] J. KRUSE, G. DETOMMASO, R. SCHEICHL, AND U. KÖTHE, *Hint: Hierarchical invertible neural*
595 *transport for density estimation and bayesian inference*, arXiv preprint arXiv:1905.10687,
596 (2019).
- [31] J. LACOTTE, Y. WANG, AND M. PILANCI, *Adaptive newton sketch: Linear-time optimization*
597 *with quadratic convergence and effective hessian dimensionality*, in International Confer-
598 ence on Machine Learning, PMLR, 2021, pp. 5926–5936.
- [32] S. LAN, S. LI, AND B. SHAHBABA, *Scaling up bayesian uncertainty quantification for inverse*
599 *problems using deep neural networks*, arXiv preprint arXiv:2101.03906, (2021).
- [33] A. T. LIN, S. W. FUNG, W. LI, L. NURBEKYAN, AND S. J. OSHER, *Alternating the popula-*
600 *tion and control neural networks to solve high-dimensional stochastic mean-field games*,
601 Proceedings of the National Academy of Sciences, 118 (2021).
- [34] A. T. LIN, W. LI, S. OSHER, AND G. MONTÚFAR, *Wasserstein proximal of gans*, arXiv preprint
602 arXiv:2102.06862, (2021).
- [35] C. LIU, J. ZHUO, P. CHENG, R. ZHANG, AND J. ZHU, *Understanding and accelerating particle-*
603 *based variational inference*, in International Conference on Machine Learning, PMLR, 2019,
604 pp. 4082–4092.
- [36] Q. LIU AND D. WANG, *Stein variational gradient descent: A general purpose bayesian inference*
605 *algorithm*, in Advances in neural information processing systems, 2016, pp. 2378–2386.
- [37] A. LIUTKUS, U. SIMSEKLI, S. MAJEWSKI, A. DURMUS, AND F.-R. STÖTER, *Sliced-wasserstein*
606 *flows: Nonparametric generative modeling via optimal transport and diffusions*, in Inter-
607 national Conference on Machine Learning, PMLR, 2019, pp. 4104–4113.
- [38] Z. LU, H. PU, F. WANG, Z. HU, AND L. WANG, *The expressive power of neural networks:*
608

- 625 *A view from the width*, in Proceedings of the 31st International Conference on Neural
626 Information Processing Systems, 2017, pp. 6232–6240.
- 627 [39] P. MOKROV, A. KOROTIN, L. LI, A. GENEVAY, J. SOLOMON, AND E. BURNAEV, *Large-scale*
628 *wasserstein gradient flows*, arXiv preprint arXiv:2106.00736, (2021).
- 629 [40] D. ONKEN, S. W. FUNG, X. LI, AND L. RUTHOTTO, *Ot-flow: Fast and accurate continuous*
630 *normalizing flows via optimal transport*, arXiv preprint arXiv:2006.00104, (2020).
- 631 [41] F. OTTO, *The geometry of dissipative evolution equations: the porous medium equation*, Com-
632 munications in Partial Differential Equations, 26 (2001), pp. 101–174.
- 633 [42] M. PILANCI AND T. ERGEN, *Neural networks are convex regularizers: Exact polynomial-time*
634 *convex optimization formulations for two-layer networks*, in International Conference on
635 Machine Learning, PMLR, 2020, pp. 7695–7705.
- 636 [43] M. PILANCI AND M. J. WAINWRIGHT, *Newton sketch: A near linear-time optimization algorithm*
637 *with linear-quadratic convergence*, SIAM Journal on Optimization, 27 (2017), pp. 205–245.
- 638 [44] D. REZENDE AND S. MOHAMED, *Variational inference with normalizing flows*, in International
639 conference on machine learning, PMLR, 2015, pp. 1530–1538.
- 640 [45] A. SAHINER, T. ERGEN, J. PAULY, AND M. PILANCI, *Vector-output relu neural network prob-*
641 *lems are copositive programs: Convex analysis of two layer networks and polynomial-time*
642 *algorithms*, arXiv preprint arXiv:2012.13329, (2020).
- 643 [46] A. M. STUART, *Inverse problems: a Bayesian perspective*, Acta numerica, 19 (2010), pp. 451–
644 559.
- 645 [47] C. VILLANI, *Topics in optimal transportation*, American Mathematical Soc., 2003.
- 646 [48] Y. WANG, P. CHEN, AND W. LI, *Projected wasserstein gradient descent for high-dimensional*
647 *bayesian inference*, arXiv preprint arXiv:2102.06350, (2021).
- 648 [49] Y. WANG, K. DENG, H. LIU, AND Z. WEN, *A decomposition augmented lagrangian method for*
649 *low-rank semidefinite programming*, arXiv preprint arXiv:2109.11707, (2021).
- 650 [50] Y. WANG, T. ERGEN, AND M. PILANCI, *Parallel deep neural networks have zero duality gap*,
651 arXiv preprint arXiv:2110.06482, (2021).
- 652 [51] Y. WANG, Y. HUA, E. CANDÉS, AND M. PILANCI, *Overparameterized relu neural networks learn*
653 *the simplest models: Neural isometry and exact recovery*, arXiv preprint arXiv:2209.15265,
654 (2022).
- 655 [52] Y. WANG, J. LACOTTE, AND M. PILANCI, *The hidden convex optimization landscape of two-*
656 *layer relu neural networks: an exact characterization of the optimal solutions*, arXiv pre-
657 print arXiv:2006.05900, (2020).
- 658 [53] L. YANG, D. SUN, AND K.-C. TOH, *Sdpnal +: a majorized semismooth newton-cg augmented*
659 *lagrangian method for semidefinite programming with nonnegative constraints*, Mathemat-
660 ical Programming Computation, 7 (2015), pp. 331–366.
- 661 [54] A. YURTSEVER, J. A. TROPP, O. FERCOQ, M. UDELL, AND V. CEVHER, *Scalable semidefinite*
662 *programming*, SIAM Journal on Mathematics of Data Science, 3 (2021), pp. 171–200.
- 663 [55] O. ZAHM, T. CUI, K. LAW, A. SPANTINI, AND Y. MARZOUK, *Certified dimension reduction in*
664 *nonlinear bayesian inverse problems*, arXiv preprint arXiv:1807.03712, (2018).
- 665 [56] X.-Y. ZHAO, D. SUN, AND K.-C. TOH, *A newton-cg augmented lagrangian method for semi-*
666 *definite programming*, SIAM Journal on Optimization, 20 (2010), pp. 1737–1765.